

Improving Pressure Robustness, Reliability, and Versatility of Solenoid-Pump Flow Systems Using a Miniature Economic Control Unit Including Two Simple Pressure Pulse Mathematical Models

Burkhard Horstkotte,[†] Erich Ledesma,[‡] Carlos M. Duarte,[†] and Víctor Cerdà^{*,‡}

Department of Global Change Research, IMEDEA (CSIC-UIB) Institut Mediterràni d'Estudis Avançats, Miquel Marqués 21, 07190 Esporles, Spain, and University of the Balearic Islands, Department of Chemistry, Carretera de Valldemossa km 7, 5, 07011 Palma de Mallorca, Spain

In this work we have systematically studied the behavior of solenoid pumps (SMP) as a function of flow rate and flow resistance. Using a new, economic, and miniature control unit, we achieved improvements of the systems versatility, transportability, and pressure robustness. A further important improvement with respect to pressure resistance was achieved when a flexible pumping tube was inserted between the solenoid pump and the flow resistance acting as a pressure reservoir and pulsation damper. The experimental data were compared with two pressure pulse models for SMP, which were developed during this work and which were well-suited to describe the SMP operation.

Solenoid micropumps (SMP) have gained considerable importance as liquid drivers in analytical flow techniques (FT) since their first application in flow systems reported by Weeks and Johnson.¹ The initial motivation for the use of SMP was miniaturization of field applicable FT systems.

SMP present an economic alternative to (multi)syringe and peristaltic pumps, typically used for flow injection analysis (FIA)² and sequential injection analysis (SIA)³ systems, respectively. They provide a semicontinuous flow with highly pronounced pulsation. It has been considered that this pulsation causes intermediate turbulent conditions in the flow manifold improving mixing of the sample and reagents in comparison with other unsegmented FT, where laminar flow conditions are typical.

While in the first works, this feature was considered as a disadvantage due to the oscillations of the detector signal, Lapa et al. proved first that mixing of reagent and sample is enhanced and sensitivity improvements of 50% are feasible.⁴ The authors further established the denomination “multipumping flow systems” (MPFS).

In contrast to syringe pumps, SMP operate continuously, which bears the potential to shorten the time of analysis or to perform

analyte from large sample volumes.^{5,6} In contrast to and in advantage over peristaltic pumps, in MPFS, each flow channel can be controlled individually. Both FIA and SIA manifold configurations have been successfully applied so far using SMP, i.e., confluent, codirectional flows, and contra-directional (aspiration and dispense), respectively.^{4,7} Analytical applications of MPFS have been reviewed in detail elsewhere.^{8–10}

However, SMP show two considerable shortcomings: they do not work reliable in the presence of gas bubbles and particulate matter affecting both the actuation of the build-in check valves and they are notably liable to flow backpressure leading to a decrease of the effective flow with increasing flow resistance. Although there is an obvious interest in the improvement of the pressure robustness and flow rate reliability, up to date, there have been hardly any efforts to complete this objective. In this work, we studied the pressure robustness of the SMP as a function of backpressure including two strategies to improve of the pressure robustness. These have been the adaptation of the activation time, made possible by the use a versatile and highly economic relay card and software control, and the use of inflatable pumping tubes to decrease the peak backpressure. We further present for the first time simple models of the pressure and flow pulse behavior as a function of pump dimensions and manifold characteristics, which were capable of explaining the observations made from the experiments undertake.

MATERIALS AND METHODS

Distilled water was used throughout. For the evaluation of flow rates, pumped volumes where quantified by weighing on an analytical balance, including compensation of the water density at ambient temperature.

The self-priming SMP from Bio-Chem Fluidics (Boston, NJ) of nominal 8 μ L, 40 μ L, and two of 25 μ L volumes were used (types

(5) Pons, C.; Santos, J. L. M.; Lima, J. L. F. C.; Forteza, R.; Cerdà, V. *Microchim. Acta* **2008**, *161*, 73–79.

(6) Pons, C.; Forteza, R.; Cerdà, V. *Anal. Chim. Acta* **2005**, *550*, 33–39.

(7) Pinto, P. C. A. G.; Saraiva, M.L.M.F.S.; Santos, J. L. M.; Lima, J. L. F. C. *Anal. Chim. Acta* **2005**, *539*, 173–179.

(8) Lima, J. L. F. C.; Santos, J. L. M.; Dias, A. C. B.; Ribeiro, M. F. T.; Zagatto, E. A. G. *Talanta* **2004**, *64*, 1091–1098.

(9) Rocha, F. R. P.; Reis, B. F.; Zagatto, E. A. G.; Lima, J. L. F. C.; Lapa, R. A. S.; Santos, J. L. M. *Anal. Chim. Acta* **2002**, *468*, 119–131.

(10) Santos, J. L. M.; Ribeiro, M. F. T.; Dias, A. C. B.; Lima, J. L. F. C.; Zagatto, E. E. A. *Anal. Chim. Acta* **2007**, *600*, 21–28.

* To whom correspondence should be addressed.

[†] IMEDEA (CSIC-UIB) Institut Mediterràni d'Estudis Avançats.

[‡] University of the Balearic Islands.

(1) Weeks, D. A.; Johnson, K. S. *Anal. Chem.* **1996**, *68*, 2717–2719.

(2) Ruzicka, J.; Hansen, E. H. *Anal. Chim. Acta* **1975**, *78*, 145–157.

(3) Ruzicka, J.; Marshall, G. *Anal. Chim. Acta* **1990**, *237*, 329–343.

(4) Lapa, R. A. S.; Lima, J. L. F. C.; Reis, B. F.; Santos, J. L. M.; Zagatto, E. A. G. *Anal. Chim. Acta* **2002**, *466*, 125–132.

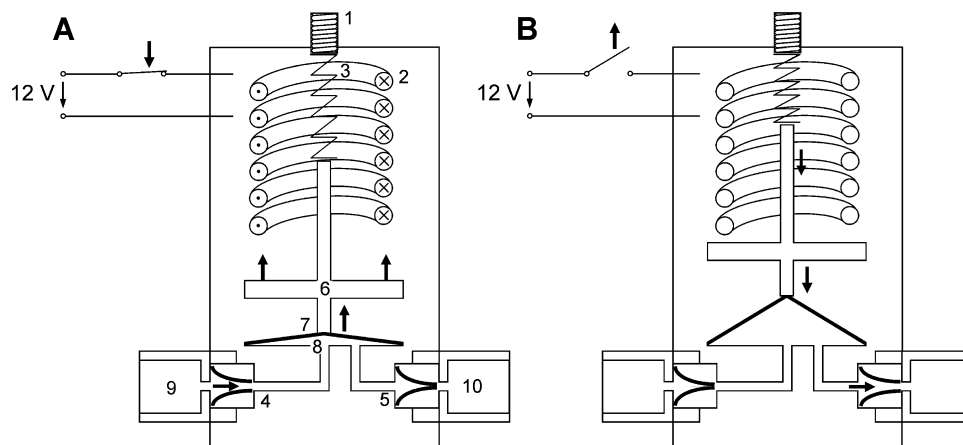


Figure 1. Scheme of the operation of the used solenoid micropumps in (A) activation (aspiration) and (B) deactivation (expulsion). Elements: 1, pretension spring; 2, solenoid; 3, spring; 4, inlet check valve; 5, outlet check valve; 6, metal core of solenoid; 7, membrane; 8, inner volume of pump; 9, inlet; 10, outlet.

P/N090SP-12-8, P/N110TP-12-40, and P/N120SP-12-25) and are denoted as pumps 1, 4, 2, and 3, respectively. In the activation state, the SMP operate in suction whereas at deactivation the pulse volume is expelled in the forward direction by the pressure exposed by a metal spring as shown schematically in Figure 1. The product specifications indicate a pressure height of 1.3 m for aspiration and 3.5 m for dispensing. Detailed specifications cited in this article can be downloaded at the producer's Web site.¹¹

For control and powering, an eight channel relay card (SERDIO8R) from EasyDAC (Glasgow, United Kingdom) was used. It allowed remote and independent control of up to eight solenoids (SMP or valves) via an RS232 serial interface. Connection of the solenoid and powering is accomplished via screw terminals, and no further equipment was required for operation. For reliable operation, parallel connection of a diode to the connected solenoid devices in reverse direction is required to deduct the induced counter-voltage at the solenoid release. The relay card is highly appropriate for miniaturization of MPFS as the dimensions are about 11 cm × 10 cm × 3 cm. A thorough description can be downloaded from the manufacture's Web site.

Three PTFE tubes of different lengths (L) and inner diameters (i.d.) were used as model flow resistances (tube 1, 49 cm, 0.2 mm i.d.; tube 2, 30 cm, 0.5 mm i.d.; and tube 3, 175 cm, 0.8 mm i.d.). For calibration of the effective pressure at a given flow rate, a Bu4S syringe pump module^{12,13} (16,000 steps, 24–1024 s for total dispense) from Crison Instruments S.A. (Alella, Barcelona, Spain) was used, equipped with a glass syringe of 5 mL from Hamilton Bonaduz AG (Bonaduz, Switzerland). Pressure measurements were performed using a Bourdon pressure gauge of 6 bar working range connected by a peek tube (20 cm, 0.8 mm i.d.) and a three-way connector between the solenoid pump and the pressure resistance. For testing the potential of pressure pulse dampers, two pieces of purple/black marked peristaltic pumping tube (2.05 mm i.d.) of 30 and 6.5 cm effective length were used.

Remote software control of the relay card as well as of the syringe pump was done via an RS232C serial interface using the AutoAnalysis 5.0 platform¹⁴ from Sciware (Palma de Mallorca, Spain) including specific dynamic link libraries (DLL) for each communication port and connected instrument.

The DLL made for the used relay card was adapted for both SMP and three-way solenoid valves. It included a calibration mode for connected SMP, definition of the mean pulse volume and minimal activation time for each relay, and the selection and definition of two of the three operation parameters (flow rate, dispense volume, and operation time) for each step and for each individual SMP. The control panels corresponding to configuration and operation instructions are shown in Figure 2, respectively. The DLL is commercially available from Sciware SL.

RESULTS AND DISCUSSION

Calibration of the Flow Resistances. For calibration of flow resistances, a smooth, nonpulsed flow was required. Therefore, a syringe pump was used. The obtained data are given in Table 1. The relation between flow rate and pressure was linear, and effective flow resistances of 0.66, 0.062, and 0.017 bar min mL⁻¹ were found corresponding to hydrodynamic diameters of tubes of 0.27, 0.42, and 0.91 mm i.d.

3.2. Calibration of the Solenoid Micropumps. For calibration, the volume of water resulting from 240 pump pulses was weighted in triplicate using an activation frequency of 2 Hz and, for both the in- and outflow of the SMP, PTFE tubes of 20 cm length and 1.5 mm i.d., respectively, which corresponded to neglectible flow resistances.

The activation time was varied between 50 and 400 ms. Longer activation times were not feasible due to low operation reliability and excessive heating of the solenoid. The results and mean pulse volumes are represented in Figure 3.

It was found that the mean pulse volume was approximately stable for activation times between 150 and 300 ms and exceeded in every case the nominal volume given by the producer: by 12% (pump 1), 21% (pump 2), 40% (pump 2), and 120% (pump 4) (P/

(11) http://www.biochemfluidics.com/pdf/micro-pumps_brochure_dn_ibpmp-01_r1.pdf, accessed February 20, 2010.

(12) Cerda, V.; Estela, J. M.; Forteza, R.; Cladera, A.; Becerra, E.; Altimira, P.; Sitjar, P. *Talanta* **1999**, *50*, 695–705.

(13) Horstkotte, B.; Elsholz, O.; Cerdá, V. *J. Flow Injection Anal.* **2005**, *22*, 99–109.

(14) Becerra, E.; Cladera, A.; Cerda, V. *Lab. Robotics Autom.* **1999**, *58*, 131–140.

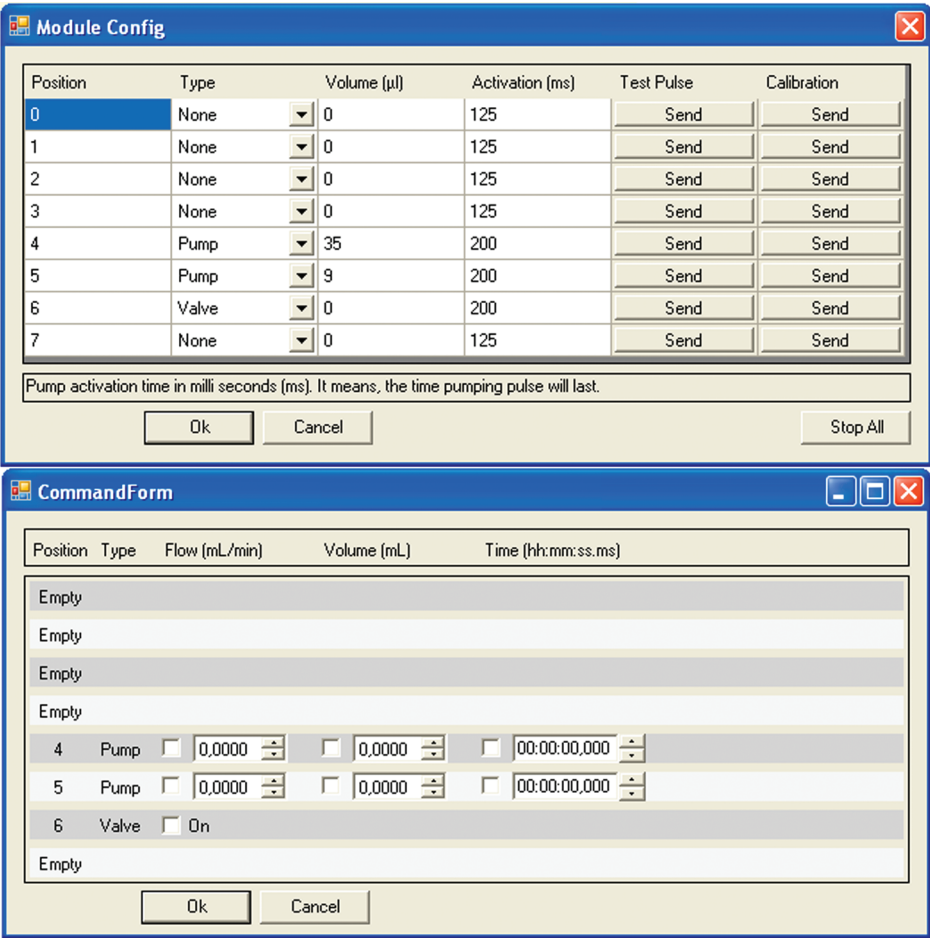


Figure 2. Configuration editor window (above) and instruction command window (below) for the software control of the used relay card using the program AutoAnalysis.

Table 1. Data from Calibration of Model Flow Resistances

flow rate [mL/min]	pressure [bar]		
	tube 1 (49 cm, 0.2 mm i.d.)	tube 2 (30 cm, 0.5 mm i.d.)	tube 3 (175 cm, 0.8 mm i.d.)
0.50	0.30		
0.60	0.35		
0.75	0.47		
1.00	0.70		
1.50	1.00		
2.50		0.15	
3.75		0.22	
5.00		0.32	0.08
6.00		0.40	0.10
7.50		0.50	0.14
pressure/flow rate [bar min mL ⁻¹]	0.659	0.0651	0.0175
hydrodynamic diameter [mm]	0.27	0.42	0.91

For pump 4, activation times below 50 ms or above 400 ms disabled pumping operation. Activation times above 250 ms lead to notable pump heating, leading to higher pulse volumes.

3.3. Pressure Pulse Model 1. To simulate the pressure pulse, a numerical flow model was created. The inner volume of the SMP (see Figure 1) can be described best by a cone, where the base is the cross section area of the inner cavity of the pump and the surface shell is the membrane elevated in its central point by attraction of the solenoid. The inner volume is therefore calculated by eq 1, where h_i is the lift of the membrane at time i .

$$V_{in,i} = \frac{1}{3} r_{pump}^2 \pi h_i$$

163

At the release of the solenoid, the pressure is equal to the spring force F applied on the inner cross section area A of the pump. The spring force is a product of the spring constant D and the sum of the initial lift h_0 and the pretension h' according eq 2. The initial lift was calculated from the calibrated pulse volume of the pump by transformation of eq 1.

$$p_0 = \frac{F_{spring}}{A_{pump}} = \frac{D(h_0 + h')}{r_{pump}^2 \pi} = \frac{D\left(\frac{3V_{pump}}{r_{pump}^2 \pi} + h'\right)}{r_{pump}^2 \pi}$$

170

N110TP-12-40). For pumps 2 and 3 (type P/N120SP-12-25), the same behavior of decreasing pulse volume with increasing activation time was found, while for pumps 1 and 4, the expulsion volume increased with the activation time. This was reduced to different responses of the rubber two check valves (see Figure 1). Because of slight differences in fabrication and abrasion, the characteristics of the pump are assumed to be determined by the weaker check valve.

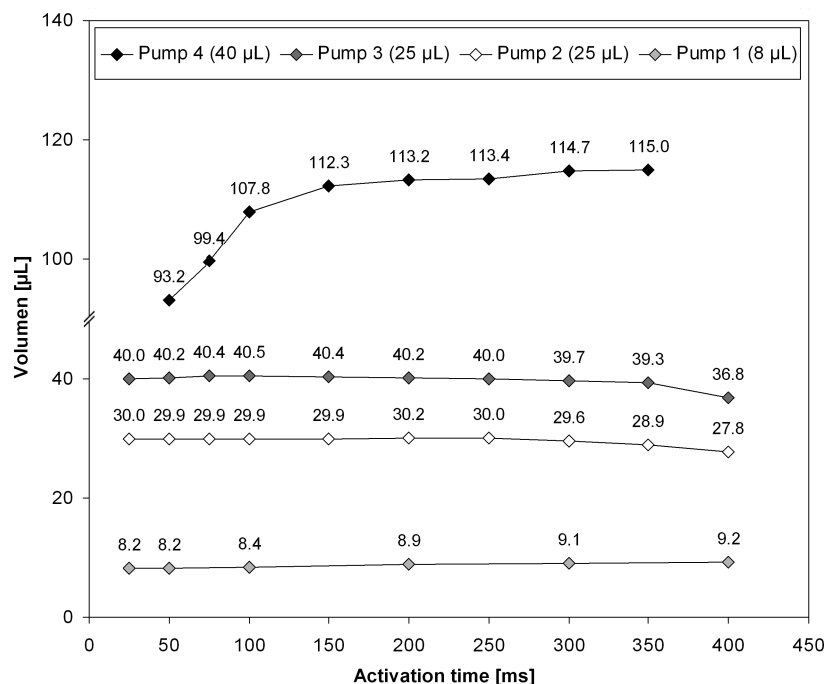


Figure 3. Dependency of mean pulse volume on the activation time (240 pulses at 2 Hz, 3-fold repetition).

The initial pressure leads to an outflow Q through the connected flow resistance characterized by tube length L and inner radius r and liquid viscosity η at a given temperature given by eq 3 (Hagen–Poiseuille equation).¹⁵

$$Q_i = \frac{p_i r^4 \pi}{8 \eta L} \quad (3)$$

The outflow leads to a spring and pressure release. The full release is reached when h_i equals 0. The membrane position and pressure after one time interval Δt are described by eqs 4 and 2, respectively. Here, we applied a time interval Δt of 10 ms for modeling.

$$h_i = h_{i-1} - \frac{1}{3} \frac{Q_i \Delta t}{r_{\text{pump}}^2 \pi} \quad (4)$$

To describe the flow conditions, the Reynold number was calculated further being the product of flow rate, radius of the flow resistance tube, liquid density, and dynamic viscosity.¹⁵

$$\text{Re}_i = \frac{Q_i r 2 \rho}{\eta} \quad (5)$$

3.4. Application of Solenoid Valves to Model Flow Resistances. The model flow resistances (tubes 1–3) were tested on the SMP for different activation times. The found mean pulse volume after expulsion of a theoretical volume of 2 mL was set in relation to the maximal found pulse volume during the former calibration, denoted further as operation efficiency (OE). The results are shown in Figure 4A–D.

With the use of an activation time of 200 ms, it was found that even for the lowest flow resistance (tube 3) the OE were significantly reduced and that efficiency loss increased with the pump size or pulse volume, respectively. In fact, the found pulse volumes fitted approximately with the nominal pulse volume of the SMP given by the producer.

For the lowest resistance, OE was about 90% (same range as the former reported¹) for pumps 1, 2, and 3 and about 40% for pump 4. For tube 3, OE values further showed to be independent from the flow rate, while for higher flow resistances, more pronounced for tube 1 than for tube 2, the OE values decreased considerably with higher flow rate. The behavior of pumps 2 and 3 were found to be similar when the pulsation frequency was used as an independent variable of data representation.

Decreasing the activation time from 200 to 50 ms but maintaining the same operation frequency improved the OE for pumps 2 and 3 for flow resistance tube 1 up to 15%. A similar behavior was found for pump 1 at operation frequencies >1.5 Hz. This improvement was reduced to the prolongation of the deactivation time and in consequence of outflow progress.

In contrast, the OE of pump 4 decreased mainly with the flow resistance with minimal effect on the flow rate. This was explained by the high volume of the SMP requiring deactivation times of several seconds for full expulsion. Leakage of the inlet SMP check valve has to be considered further. Such leakage would lead to a continuous loss over the entire pressure exhibition time.

The observations indicate that the mean flow rate is not an appropriate parameter to describe or calculate the backpressure exposed by the flow resistances but the pulse volume and pulsation frequency are the main parameters affecting the flow rate. Pons et al.⁶ recommended “periodic recalibration of the micropumps”. From the results presented here, it becomes clear that reliable off-system calibration of the SMP is not possible but has to be done within the flow system and at the aimed operation

(15) Glück, B. *Hydrodynamische und gasdynamische Rohrströmung; Druckverluste; Bausteine der Heizungstechnik*; VEB Verlag für Bauwesen: Berlin, Germany, 1998 (ISBN: 3-345-00222-1).

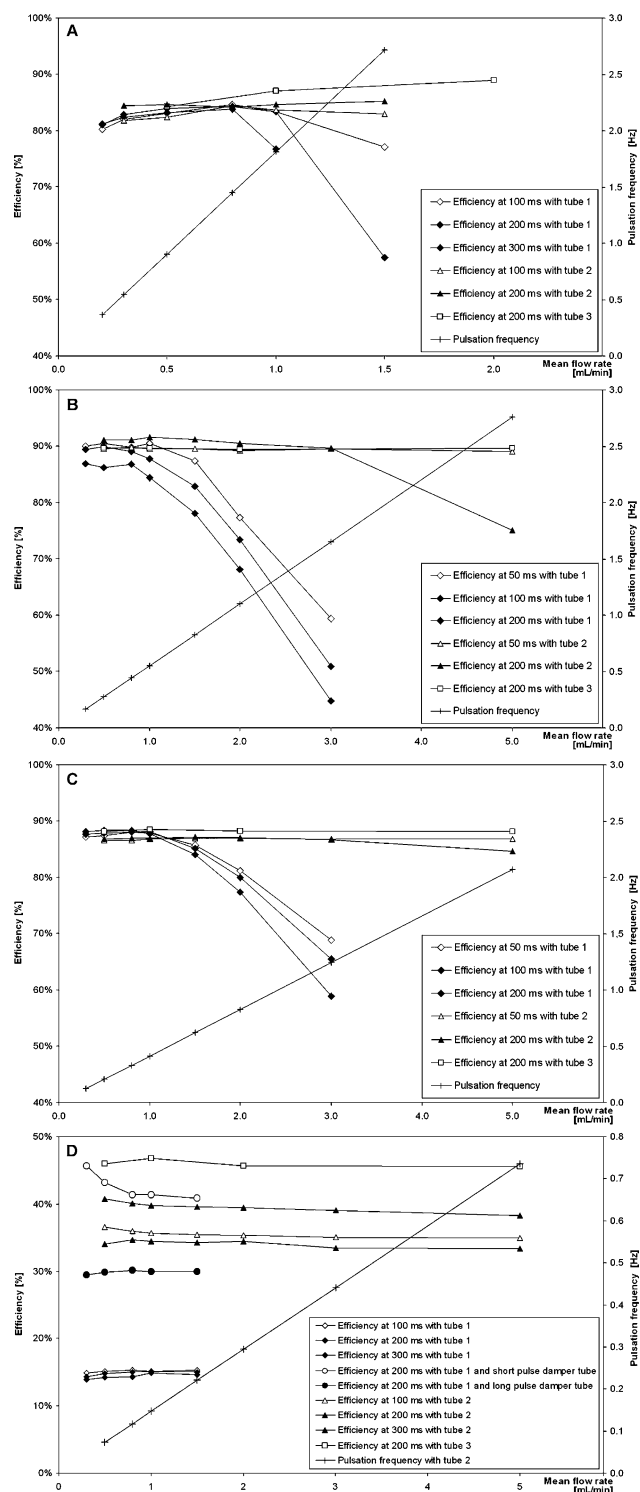


Figure 4. Dependencies between volumetric efficiency and mean flow rate for pump 1 (A), 2 (B), 3 (C), and 4 (D) for different activation times and flow resistances. In part D, the effect of peristaltic pumping tubes used as a pulsation damper on pressure robustness is shown further.

vernier caliper. The spring constant was determined to be about 2500 N/m. Further geometric dimensions measured by the vernier caliper were a prestressing of 4 mm and an inner diameter of 14 mm. The initial lift h_0 was then calculated from the pulse volume of 40 μL using eq 1.

Simulations of the pressure pulse release made with model 1 are shown in Figure 5 for pump 3 neglecting any elasticity of the flow resistance tubes. As expected, the pressure release follows a first-order lag (PT1) behavior. Since the lion share of the spring force is the result of the pretension, the pressure decrease over the pulse duration is low from 0.8 to 0.67 bar. This fact is fundamental for reliable SMP operation, and a simple way to improve the SMP pressure stability is to enhance the pretension and, if required, the operation voltage. However, break-through of the check valves and excessive solenoid heating probably limits this modification.

From Figure 5C it becomes clear why the OE of pump 3 decreases at frequencies above 0.5 Hz for tube 1. As a matter of fact, the deactivation time is not sufficiently long for the flow out of the entire pulse volume from the SMP. With the use of shorter activation times, i.e., longer deactivation times while keeping the operation frequency constant led therefore to improved operation efficiencies.

As stated, the initial pressure of pump 3 was about 0.8 bar while the producer guarantees only about 0.33 bar. To evaluate the maximal pressure applicable by the SMP, they were directly connected to the aneroid barometer, obtaining stable levels of 1.35 bar for pump 1, 1.55 bar for pumps 2 and 3, and 1.15 bar for pump 4, overcoming the stated pressure stability up to 4-fold but at the expense of an OE of zero (dispense volume = 0). The theoretical pressures at the tested flow rates considering pulse-less flow are given in Table 2. The OE started to decrease for theoretical pressures higher than 0.5 bar. It should be pointed out that with model 1 with pump 3, Reynold numbers higher than 2300 were not obtained, indicating that the pulsated flow is still laminar, which contradicts the generally stated turbulent flow conditions for MPFS.

3.5. Pressure Pulse Model 2. Elasticity of the connected tubing was neglected in pressure pulse model 1. In reality, tubing elasticity leads to a faster pulse volume expulsion, faster pressure decrease, and further delay behavior of both pressure and flow rate in the downstream tube.

In section 3.6, experiments made with an elastic pumping tube inserted between the SMP and the flow resistance will be discussed. To describe the fluid mechanics, we included the characteristics of an elastic pumping tube in a second pressure pulse model.

If an elastic cavity is inflated, the wall tension will cause the increase of the fluid pressure within. The ratio of volume increase per pressure unit is denoted compliance and is, if simplified as a linear behavior, given by eq 6.

$$C = \frac{\Delta V}{\Delta p} = \frac{V_i - V_0}{p_i - p_0} \quad (6)$$

In consequence, the pressure in the tube p_{tube} could be calculated according to eq 7.

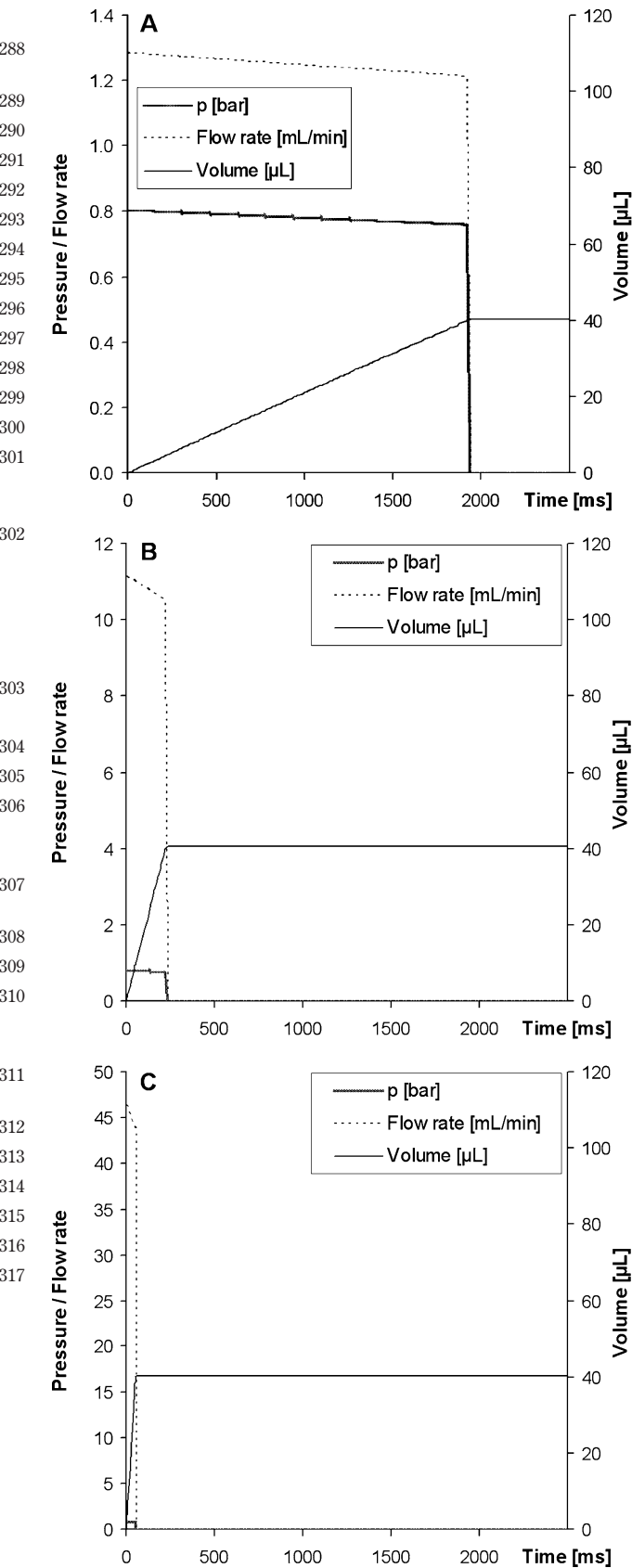


Figure 5. Modeling of the pressure and flow pulse of pump 3 for the used flow resistances (A) tube 1 (49 cm, 0.27 mm i.d.), (B) tube 2 (30 cm, 0.42 mm i.d.), (C) tube 3 (175 cm, 0.91 mm i.d.) with no tube elasticity.

$$\dot{p}_{\text{tube},i} = \frac{\Delta V}{C} = \frac{V_i - V_0}{C} \tag{7}$$

The two flow rates out of the pump into the elastic tube Q_{In} and out of the elastic tube Q_{Out} through the flow resistance were defined. Q_{Out} was calculated from the pressure in the elastic tube and the connected flow resistance analogous to eq 3. Q_{In} was calculated according eq 8 distinguishing three cases. (1) The SMP is already empty and consequently both p_{pump} and Q_{In} are zero.

(2) The pressure in the tubing and the SMP are equal so that the Q_{In} is equal to Q_{Out} . (3) The p_{pump} overcomes p_{tube} so that Q_{In} is limited by the pressure difference and the flow resistance of the outlet check valve defined by its passage radius r_{Valve} and its length L_{Valve} according to eq 3 and its time response T and Q_{Out} .

$$Q_{\text{in},i} = \begin{cases} p_{\text{pump},i} = 0 \mid = 0 \\ \text{if } p_{\text{pump},i} > p_{\text{tube},i} \mid = (p_{\text{pump},i} - p_{\text{tube},i})(1 - e^{-t/T}) \frac{r_{\text{Valve}}^4 \pi}{8\eta L_{\text{Valve}}} + Q_{\text{out},i} \\ p_{\text{pump},i} = p_{\text{tube},i} \mid = Q_{\text{tube},i} \end{cases} \tag{8}$$

The accumulating volumes of expulsion from the SMP into the elastic tube V_{In} and from the compliance elastic tube through the flow resistance V_{Out} were calculated according to eq 9.

$$V_i = Q_{i-1} \Delta t + V_{i-1} \tag{9}$$

The inner volume of the elastic tube was calculated by eq 10 being a simple balance of the initial volume, the flow out Q_{Out} , and the flow in Q_{In} .

$$V_{\text{tube},i} = V_{\text{tube},i-1} + Q_{\text{In},i-1} \Delta t - Q_{\text{Out},i-1} \Delta t \tag{10}$$

3.6. Improvement of Pressure Resistance. Increasing the elasticity of the flow resistance connected to the SMP allows a fast flow out of the pulse volume. This decreases the pulsation character of the flow and leads to a stabilized but lower pressure in the system. Since the backpressure is proportional to the 2nd power of the flow rate, smoothing the flow pulsations by an

Table 2. Theoretical Pressure for the Tested Mean Flow Rates Using the Model Flow Resistances and Found Dynamic Inner Diameters

flow rate [mL/min]	pressure [bar]		
	tube 2 (0.27 mm i.d. 49 cm)	tube 2 (0.42 mm i.d. 30 cm)	tube 3 (0.91 mm i.d. 175 cm)
0.2	0.13		
0.3	0.19	0.02	0.01
0.5	0.31	0.03	0.01
0.8	0.50	0.05	0.01
1.0	0.63	0.07	0.02
1.5	0.94	0.10	0.03
2.0	1.25	0.13	0.03
3.0	1.88	0.20	0.05
5.0		0.33	0.09

318 integral element such as an elastic pumping tube could decrease
319 the peak flow rate through the flow resistance and improve the
320 OE.

321 Since the time for liquid expulsion increases with the pulse
322 volume of the used pump, the contribution of any existing leakages
323 through the inlet check valve of the SMP would increase as well.
324 Allowing a fast flow-out against an apparently lower flow resistance
325 can therefore increase the OE because after expulsion the
326 resistance of two check valves would have to be overcome to
327 enable a counter-directional flow. By this, the solenoid membrane
328 can reach its final position of the deactivated status in less time
329 and can aspirate a full pulse volume again. On the other hand,
330 another producer of equivalent solenoid micropumps stated that
331 "it is recommended to use hard tubing for piping"¹⁶ since soft
332 tubing might absorb the pressure pulse and affect the OE of the
333 SMP.

334 For testing the potential of pressure pulse dampers, two pieces
335 of purple/black marked peristaltic pumping tube (2.05 mm i.d.)
336 of 30 and 6.5 cm effective length were used and inserted between
337 solenoid pump 4 and the model flow resistance tube 1. As shown
338 in Figure 4D, the insertion of the shorter peristaltic pumping tube
339 doubled the operation efficiency of the pump and a further
340 improvement of 10% was possible using the longer peristaltic
341 pumping tube. However, it was observed that the flow was delayed
342 and lasted several seconds after finalization of the pumping
343 operation.

344 The compliance of the elastic tube, i.e., the volumetric
345 expansions of the elastic tube in function of the inner pressure
346 was an experimental parameter. It was measured by connecting
347 the elastic tube and the former flow resistance tube 1 to the
348 syringe pump and applying different flow rates. When the flow
349 stops, the lasting flow out was collected and weighed. A linear
350 relationship between pressure, calculated from the applied flow
351 rates and resistance, and volume was found in the range of 0.3 to
352 1.2 bar, leading to a compliance of 1055 $\mu\text{L}/\text{bar}$ per meter of the
353 elastic tube.

354 It was not possible to measure neither the response time of
355 the check valve nor the flow path dimensions during the flow out.
356 Values used for the flow model 2 were estimated to be 1 mm flow
357 path length, 0.4 mm open diameter, and a delay time of 50 ms.
358 The values have influence on the flow out velocity from the SMP
359 into the elastic tube but little impact on the flow-out through the
360 flow resistance and would not affect the simulation of the
361 contribution of the elastic tube of the OE of the SMP significantly.

362 The simulation of four consecutive pressure pulses with a
363 frequency of 0.33 Hz is shown in Figure 6 for neglecting any
364 elasticity (A) and considering the 30 cm peristaltic pumping tube
365 (B) for pump 4 and the flow resistance tube 1 applying time steps
366 of 10 and 2 ms, respectively.

367 It becomes clear that a single pressure pulse is insufficient to
368 describe and explain why better OE was achieved using the elastic
369 tube. However, under repeated operation and allowing a flow out
370 after stopping the SMP operation renders higher OE values.
371 Considering further a leakage through the inlet check valve or
372 higher OE, the difference between both operation modes (with
373 and without the elastic tube) would even become more pronounced.

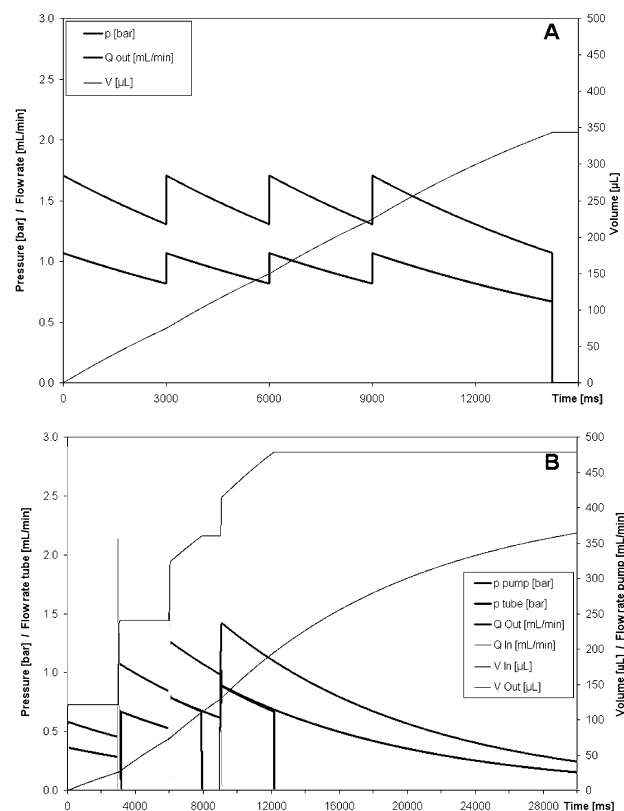


Figure 6. Modeling of the pressure and flow pulse of pump 4 for the used flow resistances (A) without elasticity included and (B) with an elastic pumping tube of 30 cm estimating a delay time of 50 ms.

Further study would be required to optimize the dimensions of peristaltic pumping tubes as a function of the pulsation volume. In fact, we did not achieve better but worse operation efficiencies for the other pumps using the elastic pumping tubes of the given dimensions.

Model 2 still shows some shortcomings: the aspiration step of the SMP was not included, and the flow resistances, delay times, and leakage loss of the check valves were not quantifiable but were estimated. However, both presented models were suited to describe the observations of SMP operation and thus present the first reported intent of SMP simulation.

CONCLUSIONS

Time adaptation and the rational use of a new economic relay card for the improvement of the operation reliability of SMP was presented. The OE being the ratio of the calibrated pulse volume and the experimental one was studied with the dependence of the connected flow resistance and activation time over a wide range of operation frequency. For the first time, the operation of SMP was simulated by pressure pulse models. The following conclusions and recommendations for future works using SMP can be made: (1) Activation and deactivation times should both exceed 150 ms. (2) The pulse volume has to be calibrated in the flow system at the desired flow rate since flow resistance and operation frequency both affect the OE considerably. (3) The use of SMP of small pulse volume at higher frequency promises higher OE than lower operation frequency using SMP with a larger pulse volume. (4) The pressure robustness of SMP passed the charac-

(16) <http://www.takasago-elec.co.jp/en/product/pump.html>, accessed February 20, 2010.

401 teristics of the producer at least twice. (5) The OE is mainly limited
402 by the required time of pulse volume expulsion. (6) The use of
403 elastic pumping tubes can render higher OE when the flow
404 resistance is high.

405 **ACKNOWLEDGMENT**

406 B.H. was funded by a JAE postdoctoral fellowship from CSIC.
407 The work was supported from Project CTQ2007-64331 funded by
408 the MEC (Spanish Ministry of Education and Science).

SUPPORTING INFORMATION AVAILABLE

This material is available free of charge via the Internet at
<http://pubs.acs.org>.

Received for review May 17, 2010. Accepted June 28,
2010.

AC101250H